Supplement of

Long-term relative decline in evapotranspiration with increasing runoff on fractional land surfaces

Ren Wang et al.

Correspondence to: Ren Wang (wangr67@mail2.sysu.edu.cn)

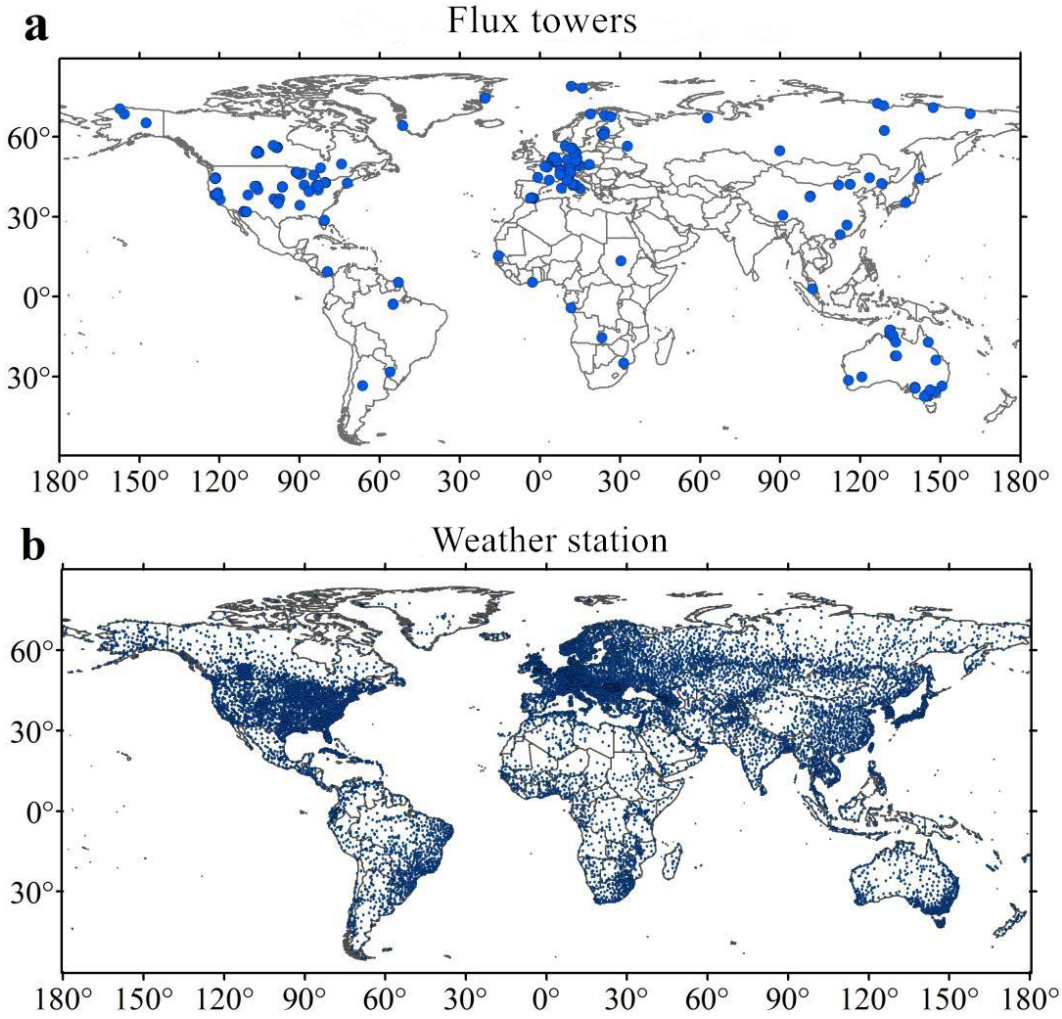

Supplementary Figure S1. Spatial distribution of (a) the flux towers and (b) the weather stations used in this study.

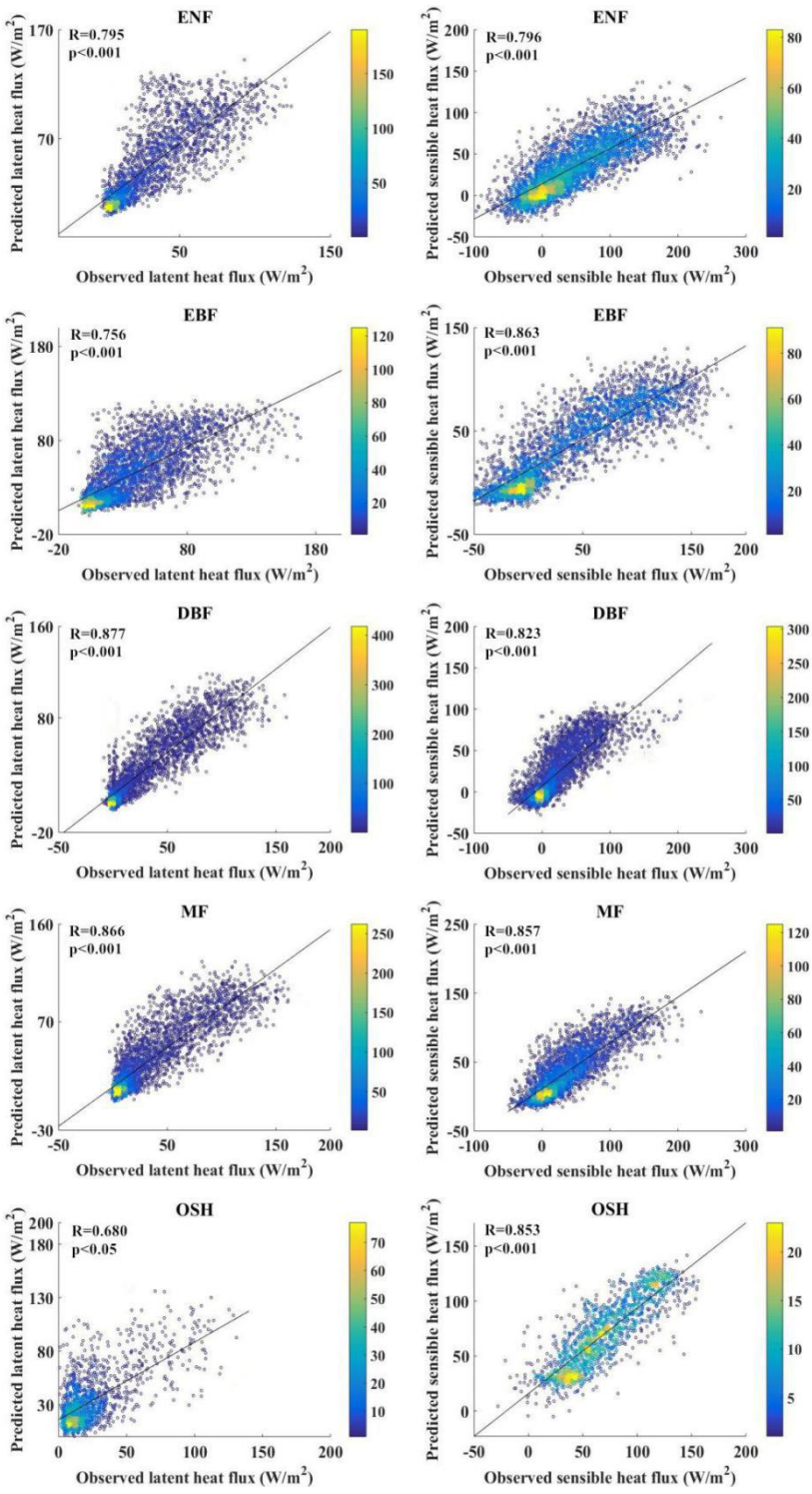

Supplementary Figure S2. Density scatter plot of the cross-validation for evergreen needleleaf forest (ENF), evergreen broadleaf forest (EBF), deciduous broadleaf forest (DBF), mixed forest (MF), and open shrublands (OSH). Samples are from five flux towers randomly selected as verification dataset.

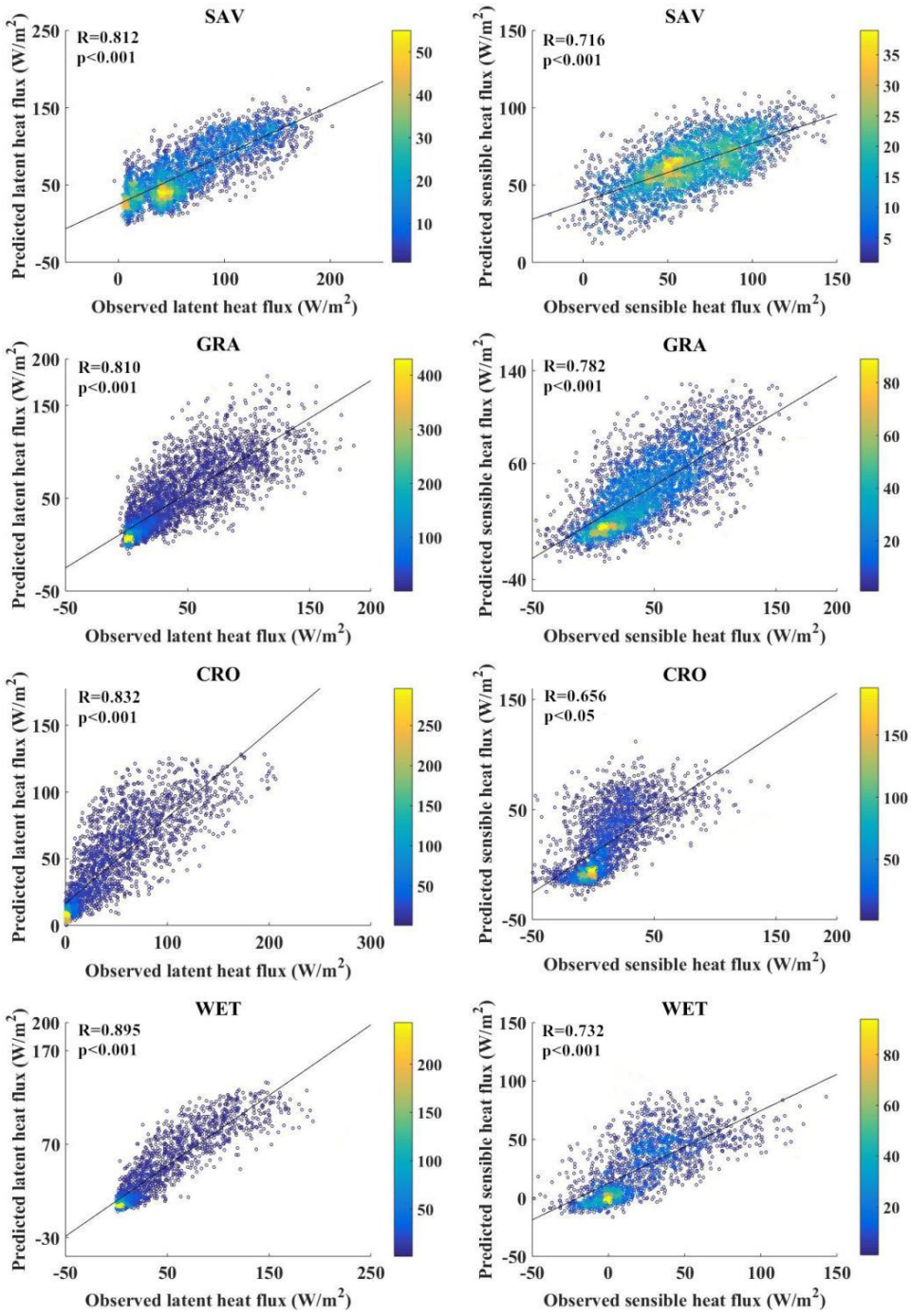

Supplementary Figure S3. Density scatter plot of the cross-validation for savannas (SAV), grasslands(GRA), croplands(CRO), and wetlands(WET). Samples are from five flux towers which were randomly selected as verification dataset.

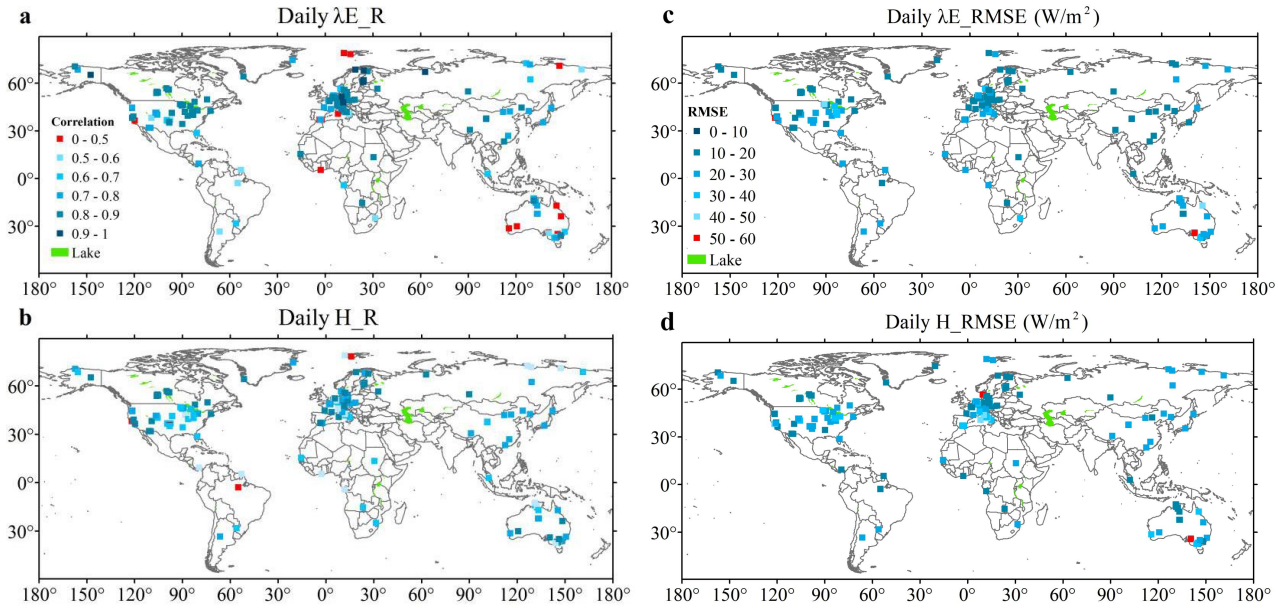

Supplementary Figure S4. Spatial distribution of correlation coefficient (R) and root mean squared error (RMSE) between the predicted latent heat flux (λE) (sensible heat flux (H)) and observed λE (H) at the daily scale for all flux towers.

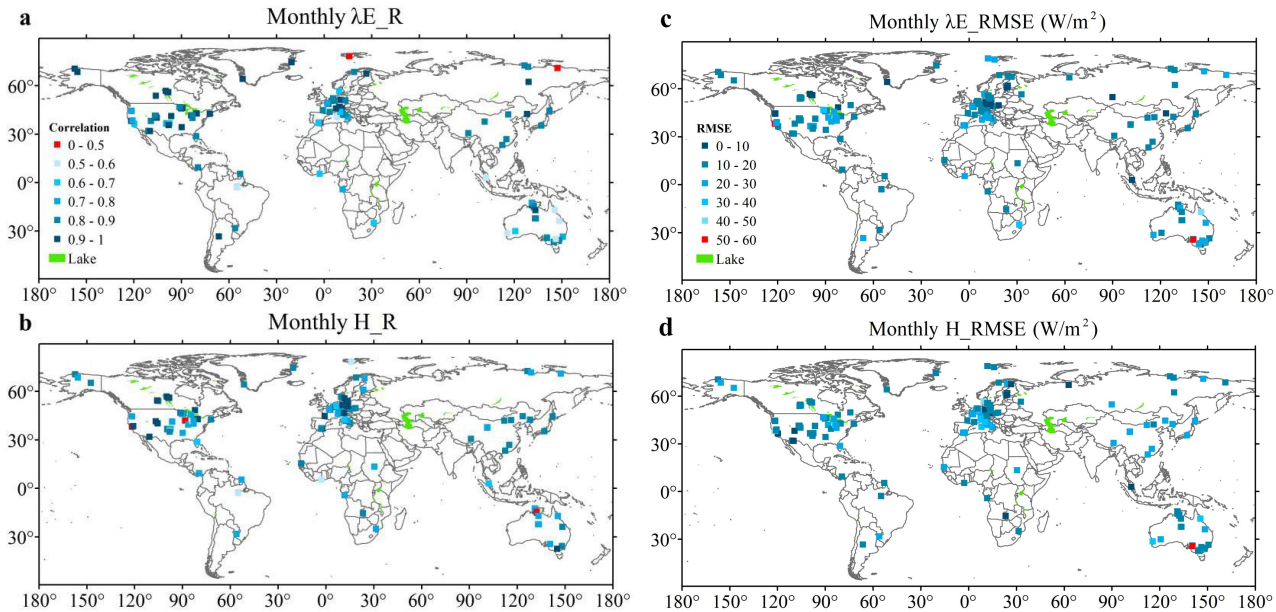

Supplementary Figure S5. Spatial distribution of R and RMSE between the predicted λE (H) and observed λE (H) at the monthly scale for all flux towers.

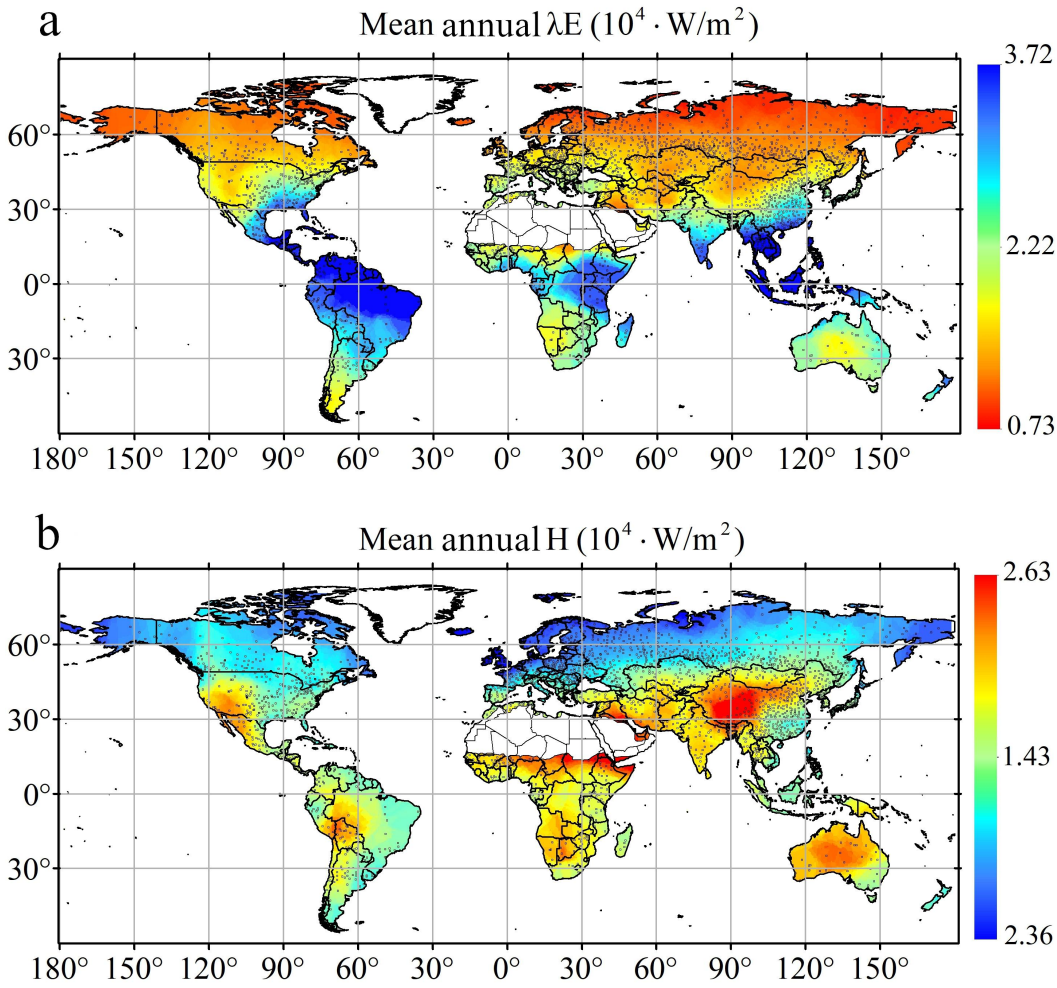

Supplementary Figure S6. Spatial distribution of the mean annual latent heat and sensible heat fluxes.

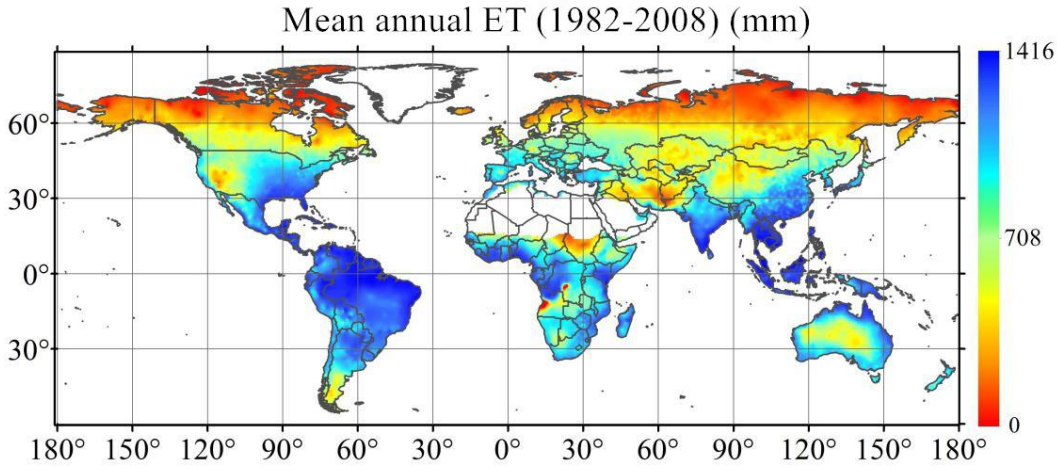

Supplementary Figure S7. Mean annual evapotranspiration (ET) during 1982–2008.

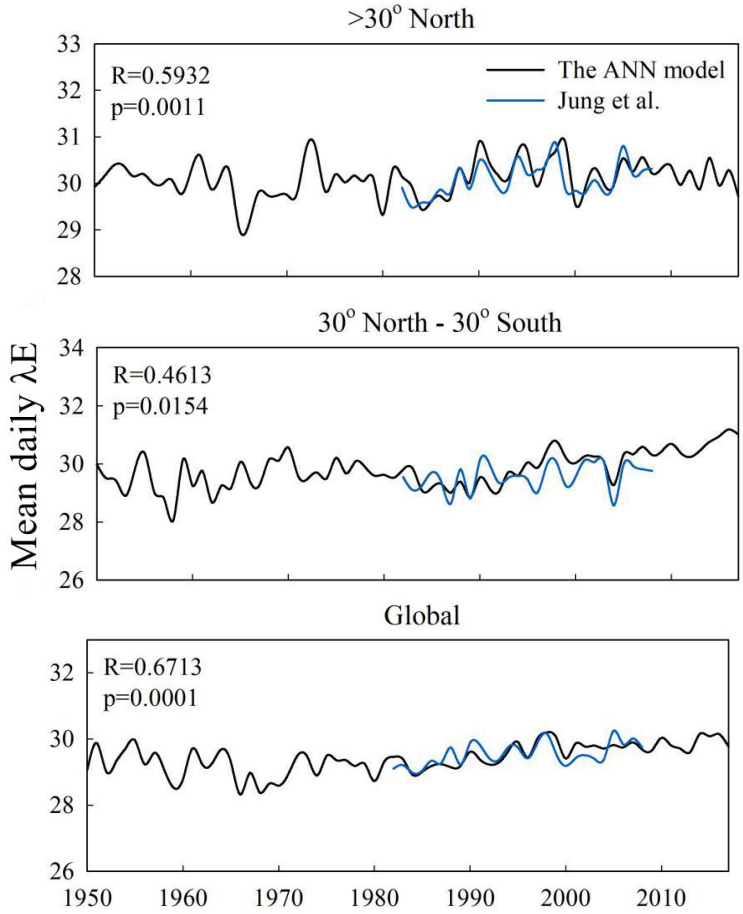

Supplementary Figure S8. Temporal changes of λE estimated by the ANN model and λE in the FLUXCOM.

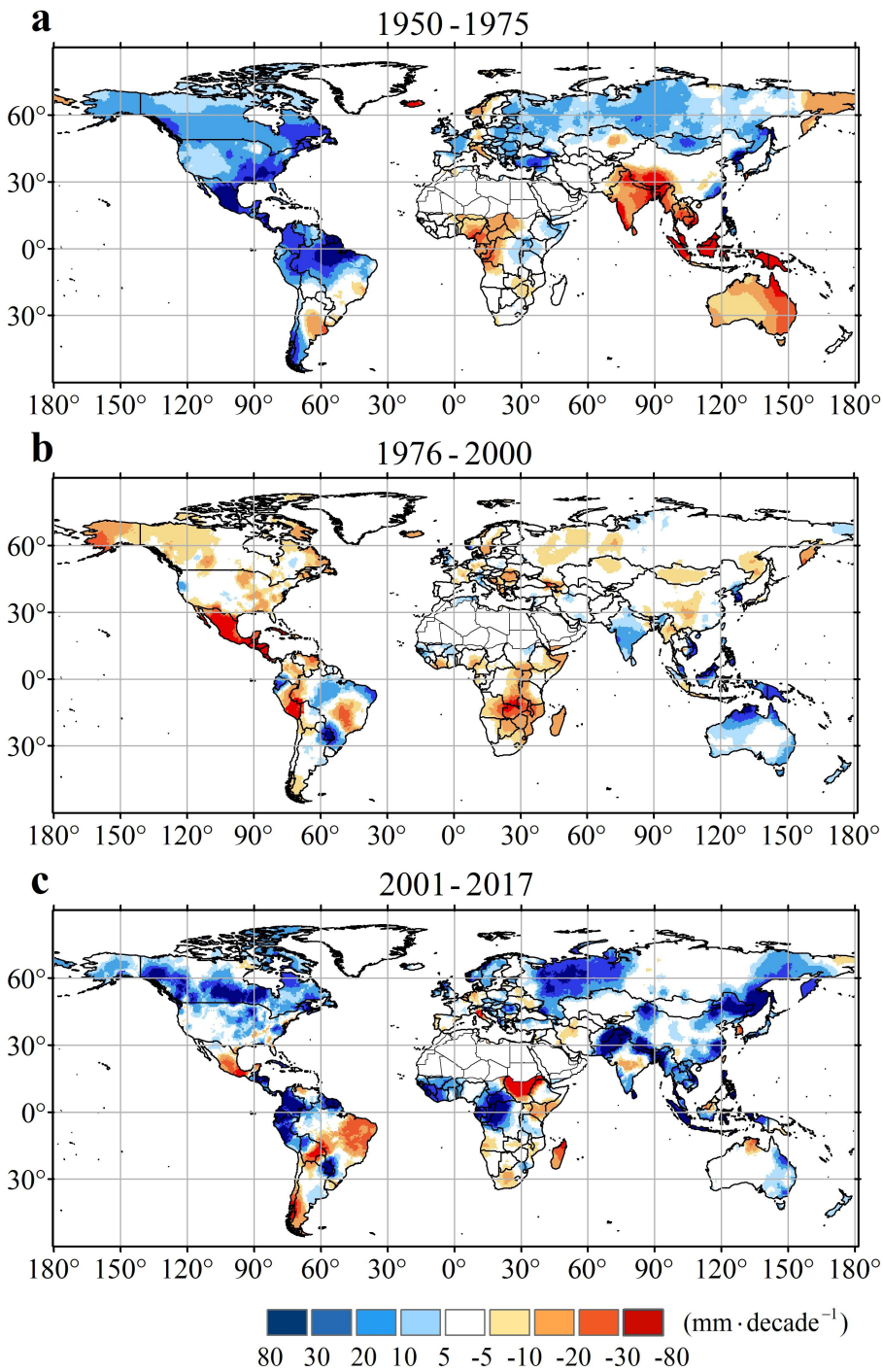

Supplementary Figure S9. Trends in annual precipitation during different historical periods.

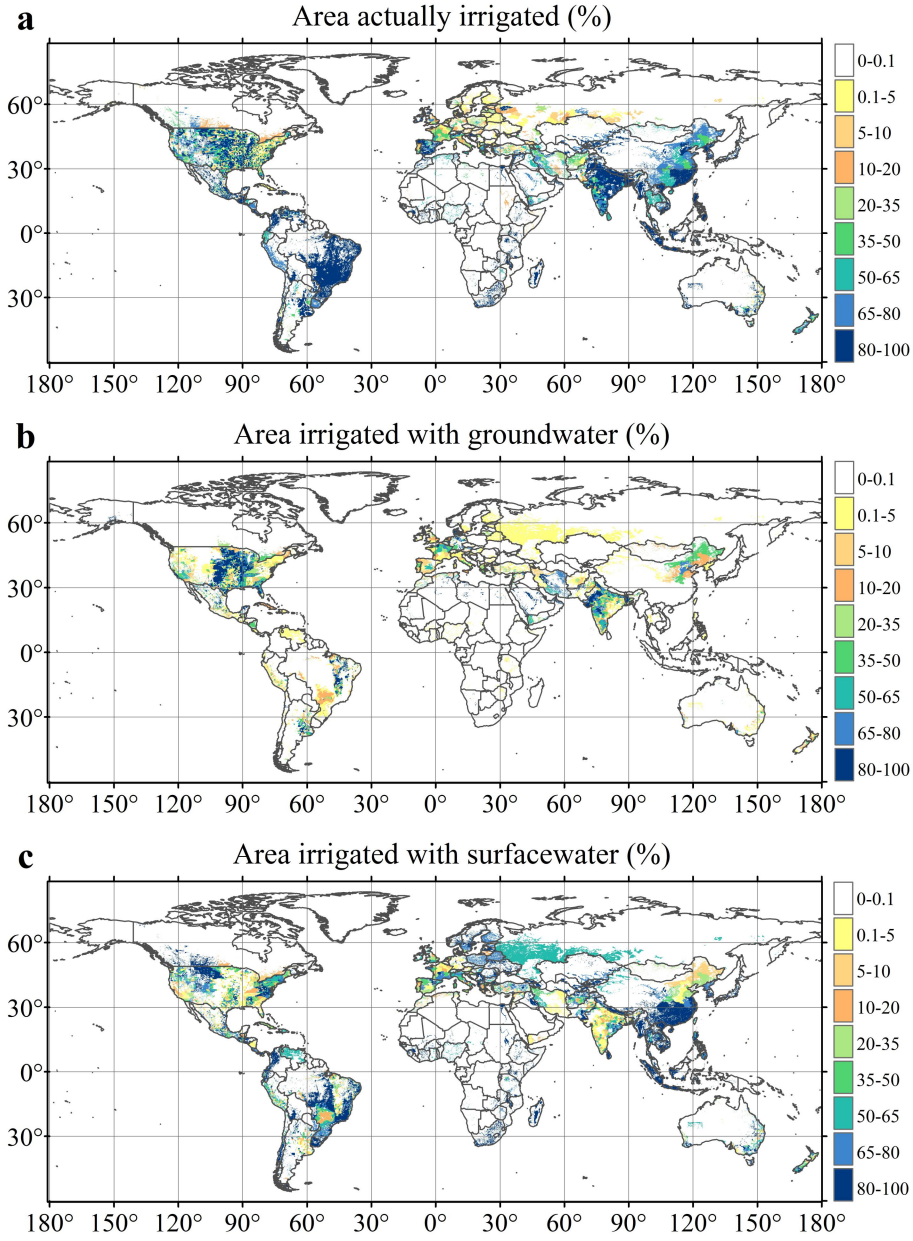

Supplementary Figure S10. Global patterns of agricultural irrigation. Global maps show percentage of the area equipped for irrigation that is (a) actually irrigated, (b) irrigated with groundwater and (c) irrigated with surface water. The base year for most countries is the 2000−2008 period.

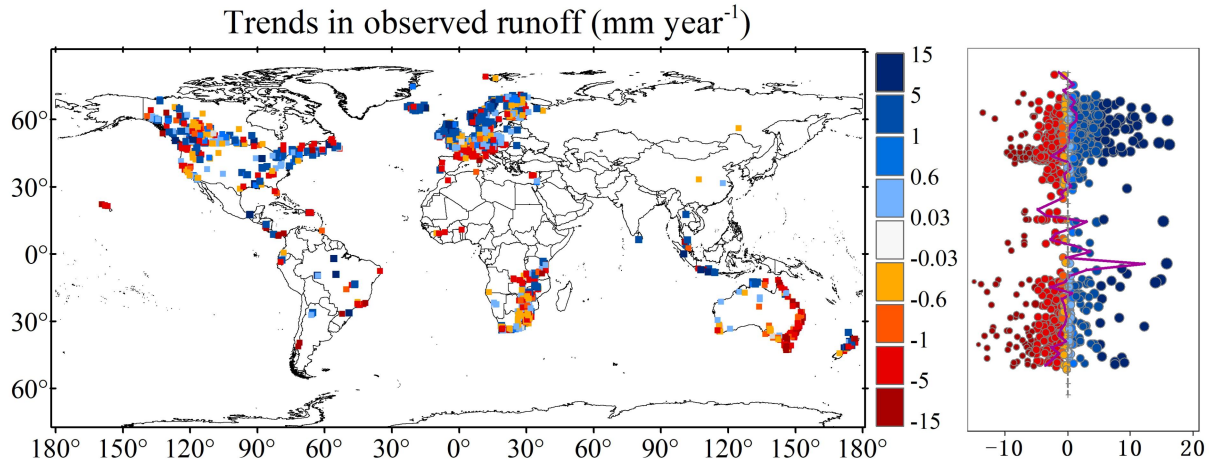

Supplementary Figure S11. Trends in observed runoff. Runoff data are from stations with a controlled watershed area of approximately 5 to 1000 km^2 with data length compiled over 20 years from the Global Runoff Data Center (GRDC). The right panel shows the runoff trends of different latitudes, and the pink curve in the panel represents the median trend of different latitude intervals.

Model training using different variable combinations

Solar radiation is a key driving force in the water cycle; however, long-term global shortwave radiation observational data are lacking at present. Therefore, this study uses daily top-of-atmosphere shortwave (SW_IN_POT) as the input for training the ANN model. Using different variable combinations as input, the sensitivity of different variables to the latent heat and sensible heat fluxes are analyzed. The results show that SW_IN_POT, relative humidity (RH), maximum temperature (Tmax), and minimum temperature (Tmin) are the main variables, while mean temperature (Tmean) and mean wind speed (Umean) are also important influencing factors (Table S1). The estimation of λE is sensitive to SW_IN_POT, RH, and Umean, while the estimation of H is sensitive to SW_IN_POT, Tmax, and Tmin. To avoid overlapping information between the long-term runoff assessed by precipitation (P) minus ET (P–ET) and the retrieved ET, P is not taken as a driving force in training the ANN model. Meanwhile, daily temperature range (DTR) has overlapping information with Tmax and Tmin, and thus it is not used for training the ANN model. List of variables and data sources for training ANN model are shown in Table S2.

Table S1. Test results of model training using different variable combinations

Combination of different variables	λE		H	
	R	RMSE (W m^{-2})	R	RMSE (W m^{-2})
{Tmax; Tmin}	0.60	36.22	0.52	43.75
{RH; Tmax; Tmin}	0.66	32.11	0.60	40.97
{RH; Tmean; Tmax; Tmin}	0.67	32.00	0.61	40.06
{RH; Tmax; Tmin; DTR}	0.67	30.89	0.62	39.48
{SW_IN_POT; Tmax; Tmin}	0.70	30.75	0.78	31.81
{SW_IN_POT; RH}	0.70	30.72	0.69	37.01
{SW_IN_POT; RH; Tmean; Tmax; Tmin}	0.74	28.80	0.72	35.8
{SW_IN_POT; RH; Tmean; Tmax; Tmin; Umean}	0.75	28.65	0.74	34.72
{SW_IN_POT; RH; Tmax; Tmin; Umean}	0.74	28.78	0.73	35.06
{SW_IN_POT; RH; Tmax; Tmin; Umean; P}	0.75	28.90	0.75	33.01
{SW_IN_POT; RH; Tmax; Umean; Tmin; P}	0.76	28.11	0.75	34.80
{SW_IN_POT; RH; Tmean; Tmax; Tmin; DTR; Umean; P}	0.77	27.12	0.74	34.34

Table S2. List of variables and data sources for training ANN model

Variables	Units	Data sources	Usage
SW_IN_POT	W/m^2	The daily integrated dataset	Input variable
Tmean	^oC	The daily integrated dataset	Input variable
Tmax	^oC	Half-hourly or hourly data	Input variable
Tmin	^oC	Half-hourly or hourly data	Input variable
VPD*	hPa	The daily integrated dataset	VPD was used to calculate RH
Umean	m/s	The daily integrated dataset	Input variable
λE	W/m^2	The daily integrated dataset	Output variable
H	W/m^2	The daily integrated dataset	Output variable

*Vapor pressure deficit (VPD) was used to calculate relative humidity.